Intermetallics 93 (2018) 72–76

Contents lists available at ScienceDirect

Intermetallics

journal homepage: www.elsevier.com/locate/intermet

Regulating kinetics of deformation-induced phase transformation in amorphous alloy composite *via* tuning nano-scale compositional heterogeneity in crystalline phase

Juan Mu[a], Jiale Wang[a], Ziyan Zhao[a], Zhengwang Zhu[b,*], Shijian Zheng[b], Zhengrong Ai[a], Yandong Wang[a,**]

[a] Key Laboratory for Anisotropy and Texture of Materials (MOE), School of Materials Sciences and Engineering, Northeastern University, Shenyang 110004, China
[b] Shenyang National Laboratory for Materials Science, Institute of Metal Research, Chinese Academy of Sciences, 72 Wenhua Road, Shenyang 110016, China

ARTICLE INFO

Keywords:
Amorphous alloy composites
Phase transformation kinetics
Compositional heterogeneity
High-energy X-ray diffraction

ABSTRACT

Nano-scale compositional heterogeneity of crystalline phase in Ti-based amorphous alloy composites (AACs) has been successfully tuned by tuning cooling rate in solidification process. And the effect of compositional heterogeneity on the kinetics of the deformation-induced phase transformation was investigated by in-situ synchrotron-based high-energy X-ray diffraction (HE-XRD) and ex-situ transmission electron microscopy. In-situ HEXRD experiments provide obvious evidence that with the decrease of the cooling rate during solidification, the critical stress of the deformation-induced phase transformation becomes lower, and the phase transformation rate becomes higher. Further high angle annular dark field-scanning electron microscopy investigation shows that the occurrence of the nano-scale Zr-lean compositional heterogeneity, which can favor the nucleation of the martensite, is the reason for the variation of the phase transformation kinetics.

1. Introduction

Deformation-induced phase transformation (PT) is a widely studied structure evolution, which plays an important role in high performance materials, such as mechanical properties and shape memory effect [1–7]. For amorphous alloy composites (AACs) with PT behaviors, plasticity as well as work hardening ability is obviously improved [8–14]. PT can induce the stress transfer and strain relaxation during deformation, which can apply advanced position for shear band initiation, favor the formation of the multiple shear bands, and finally improve the plasticity of the AACs [10,15–18]. And significant increase of the PT rate after yielding and severe plastic deformation of the crystalline phases during plastic deformation are illustrated to be the reason for the occurrence of work hardening ability. Thus the effects of PT on the mechanical properties of AACs are obvious and various.

Many issues can influence the kinetics of deformation-induced PT, such as temperature, composition, residual stress state and so on [19–21]. The most well known fact is “training” can obviously enhance the shape memory effect [2], which is attributed to that the residual stress can favor the formation of single martensitic variant and fine martensitic lath structure of deformation-induced PT. Composition is another crucial factor that can influence the PT kinetics. β- and α-stabilizing elements in Ti alloy can greatly regulate the PT kinetics [22,23]. Further studies show that besides alloying, nano-scale compositional heterogeneity also can effectively tune the kinetics of PT by favoring the nucleation of martensite [24]. For AACs with deformation-induced PT, cooling rate during rapid solidification is the key issue to regulate the compositional heterogeneity. In this work, the effect of cooling rate on the compositional cluster and further the PT kinetics of TiZr-based amorphous alloy composite were studied. The relationship between the nano-compositional cluster and PT kinetics were discussed.

2. Experimental

$Ti_{45.7}Zr_{33}Ni_3Cu_{5.8}Be_{12.5}$ (at.%) ingots were prepared by arc-melting the mixture of Zr, Ti, Cu, Ni and Be in a Ti getter high-purity argon atmosphere. Industrial sponges of Zr and Ti with purities of about 99.4 wt.% and Cu, Ni and Be with purities of 99.9 wt.% were used as raw materials. Each ingot was remelted at least four times to obtain chemical homogeneity. Rods with 3 mm, 5 mm and 12 mm in diameters were produced using the copper mold injection casting method. The structures of the specimens were studied by X-ray diffraction (XRD;

* Corresponding author.
** Corresponding author.
E-mail addresses: zwzhu@imr.ac.cn (Z. Zhu), ydwang@mail.neu.edu.cn (Y. Wang).

https://doi.org/10.1016/j.intermet.2017.11.011
Received 11 October 2017; Received in revised form 10 November 2017; Accepted 20 November 2017

Philips PW1050, Cu Ka) and scanning electron microscopy (SEM; LEO super 35) coupled with energy-dispersive spectrometry (ED). High angle annular dark field (HAADF) images were recorded using aberration-corrected scanning transmission electron microscopes (STEM; Titan Cubed 60–300 kV microscope (FEI) fitted with a high-brightness field-emission gun (X-FEG) and double Cs corrector from CEOS, and a monochromator operating at 300 kV). In order to make sure the structure homogenous, the samples for TEM and HE-XRD investigations were all cut from the central region of the as-cast samples.

In situ synchrotron-based HE-XRD experiments were conducted on the beamline 11-ID-C of the Advanced Photon Source (APS), Argonne National Laboratory (ANL). A monochromatic X-ray beam with an energy of 115 keV (wavelength 0.10801 A˚) was in situ applied to the compression test for studying the change of the scattering patterns to trace the evolution of microstructure. The size of the compressive sample is $2 \times 2 \times 4$ mm^3. The initial strain rate was 2×10^{-4} s^{-1}. Diffraction patterns were recorded by a two-dimensional (2-D) detector (Perkin Elmer amorphous silicon) installed in the front of the loaded sample.

3. Results and discussion

The microstructure of the as-cast rods with different diameters of the $Ti_{45.7}Zr_{33}Ni_3Cu_{5.8}Be_{12.5}$ alloy, indicating different cooling rates during solidification, was investigated by XRD and SEM methods. The cooling rates $\dot{T}$ achieved by different diameters can be obtained in terms of equation [25] as follows:

$$\dot{T}\left(\frac{K}{s}\right) = \frac{10}{R^2(cm)}$$

where R is the typical dimension of the sample. The cooling rates for samples with diameters of 3 mm, 5 mm and 12 mm are about 4×10^2 K/s, 2×10^2 K/s and 3×10 K/s, respectively, which means the cooling rate for the sample with 12 mm diameter is nearly one order of magnitude higher than that of the other samples. All the XRD patterns of AACs show several Bragg diffraction peaks indexed as β phase with body centered cubic structure superimpose on a broad scattering hump typical of amorphous phase. It indicates that the as-cast samples are composed of β phase and amorphous phase. The microstructural morphology of as-cast samples is investigated by SEM, as shown in Fig. 1. The β-phase dendrites with dark contrast are homogenously dispersed in amorphous matrix. The distinguish among the samples with different diameters is the size of the dendrite. After analyzing the SEM images, the size of dendrites was measured to be 10–35 μm, 20–50 μm, 40–90 μm for the samples with 3 mm, 5 mm and 12 mm in diameter, respectively. With increasing the diameter, the morphology of dendrites is well developed and coarsened, as shown in Fig. 1. It is interesting that the volume fraction of dendrites keeps almost constant for all the samples, measured to be 48% with an error of 1%. It is indicated that the coarsening of dendrites in the current system occurred in the early solidification process.

In order to study the microstructure, especially the compositional heterogeneity, of the TiZr-based AACs with different diameters, transmission electron microscopy (TEM) was used to observe the initial microstructure of dendrites. Fig. 2 is the high angle annular dark field-scanning electron microscopy (HAADF-STEM) image of the dendrite in the AACs with the electron beam along the $[100]_\beta$ direction. The bright spots indicate atom columns and the intensity of spots is proportional to the atomic number of the atom composing the columns in a HAADF image. As increasing the diameters of the samples, the compositional fluctuation, indicating by the high image contrast, becomes obvious. Especially for the sample with 12 mm diameter, nano domains with heavy atoms (noted as solid circles) or light atoms (noted as dashed circles) are both distributed randomly. Considering the atomic number of the elements in the alloy, the heavy zone would be rich in Zr. The existence of two kinds of heavy-atom (Zr) -rich and light-atom (Ti, Ni or Cu) -rich nanodomains indicates the heterogeneous nature of the parent phase β in the sample with 12 mm diameter. And the scale of the compositional non-uniformity in β phase matches the scale of the martensitic nanodomains [17]. However, the composition is generally homogenous for the samples with 3 mm and 5 mm diameters. These results illustrate that the compositional heterogeneity in dendrite can be effectively tuned by tuning cooling rate of the solidification process.

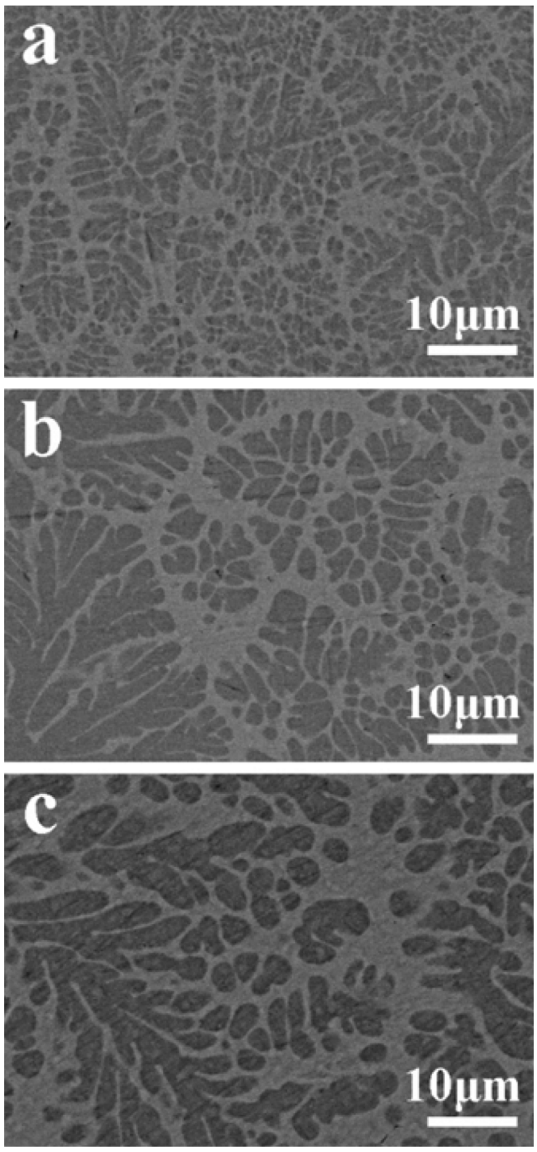

Fig. 1. SEM micrographs of the as-cast Ti-based AACs with different diameters, (a) 3 mm, (b) 5 mm and (c) 12 mm.

In-situ HE-XRD was used to investigate the deformation-induced PT kinetics of the AACs with different cooling rates. The evolution of one-dimensional (1-D) diffraction profiles along the loading direction (LD) as a function of stress is shown in Fig. 3. The profiles in the LD are chosen to describe the structure evolution since the LD was proved to be the most sensitive direction for the deformation-induced PT of the current composites [15]. As shown in Fig. 3, all samples with different diameters show the mixture of β phase and amorphous phase, which is consistent with the XRD and SEM results. With increasing loading stress, the Bragg diffraction peaks corresponding to β phase in the LD profiles shift to higher angles because of internal compressive stress. When the loading stress reaches the critical stress of the PT, a tiny peak with 2θ located at about 4° corresponding to $(200)_{\alpha''}$ appears in the profile [26], which indicates that the deformation-induced PT